NONLINEAR ROCKING MOTIONS. II: OVERTURNING UNDER RANDOM EXCITATIONS

By H. Lin[1] and S. C. S. Yim,[2] Member, ASCE

ABSTRACT: Rocking responses of rigid objects under combined deterministic and stochastic excitations of arbitrary relative intensities are examined from a fully probabilistic perspective. The associated Fokker-Planck equation is derived and numerically solved by a path-integral solution procedure to obtain the joint probability density functions (JPDFs). The evolutions and the steady states of the JPDFs are employed to elucidate the global behavior of the rocking responses. As found in the companion paper, numerical results confirm that the presence of stochastic excitation bridges the domains of attraction of coexisting responses, and that overturning attractors are of the greatest relative stability. Thus, all rocking response trajectories that visit near the heteroclinic orbit will eventually lead to overturning under the influence of stochastic excitation. A rapid leakage of the probability (mass) out of the "safe" (bounded, chaotic) domain to the overturning regime implies weak stability of the chaotic attractor. Using mean first-passage time as a performance index, sensitivity of rocking responses to system parameters and (non)stationarity of the stochastic excitation is also investigated.

INTRODUCTION

Rigid rocking object models incorporating the effects of environmental random disturbances in their response behavior have been of great interest to engineers. As shown in Lin and Yim (1996), the behaviors of periodically excited rocking response can be highly nonlinear. Addition of small amount of stochasticity in the excitation further complicates the analyses.

Several analytical studies of the stochastic response of rigid rocking blocks have appeared in the literature. Spanos and Koh (1986) employed a statistical linearization technique to examine the stochastic rocking of a rigid rectangular block on Winkler's foundation due to nonstationary foundation shaking. Koh (1986) further studied this problem through simulation and estimated the probability of no toppling. Iyengar and Manohar (1991) investigated the stochastic rocking behavior under simultaneous horizontal and vertical white noise excitations. By approximating the impact-induced energy dissipation by viscous damping, the corresponding Fokker-Planck equation was developed. Further assuming that the rigid object does not overturn under weak noise disturbance, an approximate stationary solution of the probability density function (PDF) was obtained. Overturning of the object was examined via first-passage failure. In another probabilistic analysis on the stochastic rocking response carried out by Dimentberg et al. (1993), the base excitations were modeled as white noise in both horizontal and vertical directions, and both freestanding and anchored objects were considered. By applying a quasi-conservative averaging technique, stochastic equations governing the motion were solved using a semianalytical procedure. They showed that the presence of vertical excitation, with intensity about one-half of that of the horizontal excitation, may increase the probability of toppling by 30–40%. In addition, they also found that, similar to the statistical results obtained by Yim et al. (1980), larger blocks are more stable than smaller ones of identical geometric proportion.

In Lin and Yim (1996), an investigation on a periodically excited rocking system with small random perturbations was conducted to demonstrate the intrinsic properties of various types of rocking responses (e.g., periodic, chaotic, and noisy chaotic) based on an analytical approach using the stochastic Melnikov process and average flux. In this paper, the limitations on small random perturbation intensity, large slenderness ratio of the rigid object, determinism of initial conditions, and stationarity of the excitation required in the companion paper are relaxed. The rocking behaviors of rigid objects subjected to combined deterministic and (not necessarily small) stochastic excitations are studied from a fully stochastic perspective. In particular, the large slenderness ratio (piecewise linear) constraint of the rigid object is removed here, and a fully nonlinear rocking model is employed to examine the sensitivity of the stochastic rocking response to the slenderness ratio. A unified mathematical representation of rocking behaviors subjected to combined deterministic and stochastic excitations is formulated by introducing an excitation parameter γ with the total input energy fixed. By varying this parameter from zero to one, various degrees of determinicity/stochasticity of the excitations can be performed, and their effects on rocking responses are examined. The Fokker-Planck equation corresponding to the rocking system is derived and solved semianalytically using a path-integral solution procedure. Global information of the system behavior is demonstrated via the evolution of the resulting joint probability density functions (JPDFs, or simply PDFs for simplicity). Stability of the stochastic rocking response is evaluated by estimating the mean first-passage time. Using this performance index, a sensitivity study is conducted on system parameters as well as the (non)stationarity of stochastic excitation.

PHYSICAL MODEL

The rocking response of a rigid object with arbitrary slenderness ratio subjected to combined deterministic and stochastic excitations can be formulated as in Yim et al. (1980)

$$I_0\ddot{\theta} + MRa_{gx} + MgR\sin(\theta_{cr} - \theta) = 0, \quad \theta > 0 \tag{1}$$

and

$$I_0\ddot{\theta} + MRa_{gx} - MgR\sin(\theta_{cr} + \theta) = 0, \quad \theta < 0 \tag{2}$$

Eqs. (1) and (2), respectively, represent nonslipping positive and negative rocking angles about the centers of rotation O and O'. Note that I_0 = moment of inertia about O or O'; M = mass; a_{gx} = horizontal base acceleration; R = distance from O to the center of mass; and $\theta_{cr} = \cot^{-1}(H/B)$ = critical (static overturning) angle, where H and B = height and width of the object. Impact-induced energy loss (or damping) is accounted

[1]Res. Assoc., Dept. of Civ. Engrg., Oregon State Univ., Corvallis, OR 97331.

[2]Assoc. Prof., Dept. of Civ. Engrg., Oregon State Univ., Corvallis, OR.

Note. Associate Editor: John Tassoulas. Discussion open until January 1, 1997. Separate discussions should be submitted for the individual papers in this symposium. To extend the closing date one month, a written request must be filed with the ASCE Manager of Journals. The manuscript for this paper was submitted for review and possible publication on August 3, 1995. This paper is part of the ***Journal of Engineering Mechanics***, Vol. 122, No. 8, August, 1996. ©ASCE, ISSN 0733-9399/96/0008-0728–0735/$4.00 + $.50 per page. Paper No. 11321.

for by restitution coefficient, e, which relates the angular velocities before and after impact (Yim et al. 1980)

$$\dot{\theta}(t^+) = e\dot{\theta}(t^-), \quad 0 \le e \le 1 \tag{3}$$

where t^- (t^+) = time just before (after) impact. In this study, a general form of the horizontal base excitation including both deterministic and stochastic components is given by

$$a_{gx}(t) = \gamma a \cos(\omega t + \phi) + I(t)\sqrt{1 - \gamma^2} f(t) \tag{4}$$

where a, ω, and ϕ = amplitude, frequency, and phase shift of the periodic excitation, respectively. $I(t)$ represents an intensity-time function that characterizes the time-dependent variation (thus nonstationary) of the intensity of stochastic excitation. In the limit as $I(t)$ approaches a constant, stationary stochastic excitation is recovered. Stochastic excitation $f(t)$ describes a band-limited noise disturbance, which can be obtained by linearly filtering a white noise process

$$\ddot{f} + \beta\dot{f} + \Omega_0^2 f = \xi(t) \tag{5}$$

where β and Ω_0 = bandwidth parameter and natural frequency of the filter; and ξ = a zero-mean delta-correlated white noise with noise intensity κ

$$E[\xi(\tau)] = 0 \tag{6a}$$

$$E[\xi(\tau)\xi(\tau')] = \kappa\delta(\tau - \tau') \tag{6b}$$

the spectrum associated to the filter [(5)] is given by

$$S_f(\omega) = \frac{S_0}{(\omega^2 - \Omega_0^2)^2 + \beta^2\omega^2} \tag{7}$$

It is seen that the degree of stochasticity of the rocking excitation (hence the response) is completely governed by γ, which may vary from 0 to 1. In the limit $\gamma = 0$ or 1, the system becomes purely deterministic or stochastic, respectively. For convenience of analysis, (1) and (2) are normalized by I_0, and (1) and (2) can be rewritten as

$$\ddot{\theta} + \frac{\alpha^2}{g} a_{gx} + \alpha^2 \sin(\theta_{cr} - \theta) = 0, \quad \theta > 0 \tag{8}$$

and

$$\ddot{\theta} + \frac{\alpha^2}{g} a_{gx} - \alpha^2 \sin(\theta_{cr} + \theta) = 0, \quad \theta < 0 \tag{9}$$

where $\alpha^2 = MgR/I_0$.

PROBABILISTIC ANALYSIS

A probability-domain approach is introduced in this section to demonstrate the stochastic behaviors of the rocking response. An analysis will be conducted via the Fokker-Planck equation and its semianalytical path-integral solution. The resulting joint probability density function (JPDF) is used to compute the mean first-passage time for system performance evaluation.

Fokker-Planck Equation

Probabilistic aspect of rocking responses under combined deterministic and stochastic excitations can be examined via the solutions to a partial differential equation called the Fokker-Planck equation (FPE). As shown in the previous section, response behaviors of the rocking system are characterized by two equations governing the motion and one equation governing the impacts at zero crossings. Thus, the corresponding FPE in state space can be obtained by setting four state variables

$$\mathbf{X} = [x_1\ x_2\ x_3\ x_4]^T = [\theta\ \dot{\theta}\ f\ \dot{f}]^T \tag{10}$$

and the associated FPEs for $x_1 > 0$ and $x_1 < 0$, are given by

$$\frac{\partial P(\mathbf{X}, t)}{\partial \tau} = -\frac{\partial}{\partial x_1}\{x_2 P(\mathbf{X}, t)\} - \frac{\partial}{\partial x_2}\left\{\left[-\alpha^2 \sin(\theta_{cr} - x_1) - \frac{\alpha^2\gamma a}{g} \cdot \cos(\omega t + \phi) - \frac{\alpha^2}{g} I(t)\sqrt{1 - \gamma^2} x_3\right] P(\mathbf{X}, t)\right\} - \frac{\partial}{\partial x_3}\{x_4 P(\mathbf{X}, t)\} - \frac{\partial}{\partial x_4}\{(-\beta x_4 - \Omega_0^2 x_3) P(\mathbf{X}, t)\} + \frac{\kappa}{2}\frac{\partial^2}{\partial x_4^2} P(\mathbf{X}, t) \tag{11}$$

and

$$\frac{\partial P(\mathbf{X}, t)}{\partial \tau} = -\frac{\partial}{\partial x_1}\{x_2 P(\mathbf{X}, t)\} - \frac{\partial}{\partial x_2}\left\{\left[\alpha^2 \sin(\theta_{cr} + x_1) - \frac{\alpha^2\gamma a}{g} \cdot \cos(\omega t + \phi) - \frac{\alpha^2}{g} I(t)\sqrt{1 - \gamma^2} x_3\right] P(\mathbf{X}, t)\right\} - \frac{\partial}{\partial x_3}\{x_4 P(\mathbf{X}, t)\} - \frac{\partial}{\partial x_4}\{(-\beta x_4 - \Omega_0^2 x_3) P(\mathbf{X}, t)\} + \frac{\kappa}{2}\frac{\partial^2}{\partial x_4^2} P(\mathbf{X}, t) \tag{12}$$

respectively. Note that $P(\mathbf{X}, t)$ denotes the PDF at position $\mathbf{X}$ at time t, $[x_2, -\alpha^2 \sin(\theta_{cr} - x_1) - (\alpha^2\gamma a/g)\cos(\omega t + \phi), x_4, -\beta x_4 - \Omega_0^2 x_3]^T$ and $[x_2, \alpha^2 \sin(\theta_{cr} + x_1) - (\alpha^2\gamma a/g)\cos(\omega t + \phi), x_4, -\beta x_4 - \Omega_0^2 x_3]^T$ are the drift vectors. Coefficient $\kappa/2$ is the only nonzero entry in the four-by-four diffusion matrix (Risken 1984). Note that transition of PDF from the positive displacement subdomain to the negative displacement subdomain, and vice versa, is accompanied by a reduction of the velocity magnitude [(3)]. Thus, the PDF of the rocking response is fully characterized by (11) and (12), together with the impact governed by (3).

Eqs. (11) and (12) are second-order partial differential equations of the hyperbolic type. Closed form solutions do not exist in general. To demonstrate the evolution of the PDF, a path-integral solution procedure is employed in this study to numerically solve the FPE.

Path-Integral Solution

In the path-integral solution procedure, the traveling path of the PDF in the probability space is discretized into a large number of infinitesimal segments. Each segment represents an elemental time propagation between two consecutive states in the corresponding Markov process. The short-time propagation is approximated by a time-dependent Gaussian distribution called the short-time PDF, and the mean and variance of which are determined by the drift vector and the diffusion matrix, respectively. The PDF at the succeeding state can be obtained through the propagation, and the PDF at a desired state can be obtained by applying the short-time propagation iteratively.

The short-time probability density functions, $G(\mathbf{X}', \mathbf{X}, t; dt)$, for corresponding probability subdomains of (11) and (12) are given by Wissel (1979)

$$G(\mathbf{X}', \mathbf{X}, t; dt) = (2\pi\ dt)^{-4} \frac{1}{\sqrt{\kappa}} \exp \cdot\left[-\frac{dt}{2\kappa}\left(-\beta x_4 - \Omega_0^2 x_3 - \frac{x_2' - x_2}{dt}\right)^2\right] \delta\left(x_4 - \frac{x_3' - x_3}{dt}\right) \times \delta\left[-\alpha^2 \sin(\theta_{cr} - x_1) - \frac{\alpha^2\gamma a}{g}\cos(\omega t + \phi) - \frac{\alpha^2}{g} I(t)\sqrt{1 - \gamma^2} x_3\right] \delta\left(x_2 - \frac{x_1' - x_1}{dt}\right), \quad x_1 > 0 \tag{13}$$

and

$$\mathbf{G}(\mathbf{X}', \mathbf{X}, t; dt) = (2\pi\, dt)^{-4} \frac{1}{\sqrt{\kappa}} \exp$$

$$\cdot\left[-\frac{dt}{2\kappa}\left(-\beta x_4 - \Omega_0^2 x_3 - \frac{x_2' - x_2}{dt}\right)^2\right] \delta\left(x_4 - \frac{x_3' - x_3}{dt}\right)$$

$$\times \delta\left[\alpha^2 \sin(\theta_{cr} + x_1) - \frac{\alpha^2 \gamma a}{g} \cos(\omega t + \phi)\right.$$

$$\left. - \frac{\alpha^2}{g} I(t)\sqrt{1 - \gamma^2} x_3\right] \delta\left(x_2 - \frac{x_1' - x_1}{dt}\right), \quad x_1 < 0 \tag{14}$$

where $\mathbf{X}'$ and $\mathbf{X}$ = poststate and prestate, respectively. Eqs. (13) and (14) are in the form of a degenerate Gaussian distribution. The degeneracy is caused by the complete correlation between x_1 and x_2 and x_3 and x_4 (Stratonovich 1967), which is represented by the Dirac delta functions in (13) and (14). The PDF at a desired state is given by

$$P(\mathbf{X}, t) = \lim_{\substack{dt \to 0 \\ N \to \infty \\ Ndt \to t - t_o}} \prod_{i=0}^{N-1} \int \cdots \int$$

$$\cdot \exp\left[-dt \sum_{j=0}^{N-1} G(\mathbf{X}_{j+1}, \mathbf{X}_j, t_j; dt) P(\mathbf{X}_o, t_o)\right] d\mathbf{X}_i \tag{15}$$

where $P(\mathbf{X}_o, t_o)$ = initial probability distribution

$$P(X_o, t_o) = P(x_{1o}, x_{2o}, x_{3o}, x_{4o}) \tag{16}$$

in which x_{1o} and x_{2o} = initial displacement and velocity of the rocking model; and x_{3o} and x_{4o} = initial conditions for the linear filter, respectively. If the initial conditions for the system are deterministic, (16) can be specified as

$$P(\mathbf{X}_o, t_o) = \delta(x_1 - x_{1o})\delta(x_2 - x_{2o})\delta(x_3 - x_{3o})\delta(x_4 - x_{4o}) \tag{17}$$

The path-integral solution procedure converges to the exact solution in the limit $N \to \infty$ and $dt \to 0$ in (15).

Based on the path sum (or discrete lattice representation) of the path integral, this procedure can be numerically evaluated (Wehner and Wolfer 1983). Propagation of the PDF between consecutive states is described by the corresponding segment in the discretized mean path in probability space. The probability domains at the ends of the segments, i.e., prestate and poststate, are discretized into $N_d \times N_d \times N_f \times N_f$ elements. Accordingly, the short-time PDF corresponding to the transitions between consecutive states, $G(\mathbf{X}', \mathbf{X}, t; dt)$, can be discretized in to a transition tensor, $\mathbf{\Gamma}(t; dt)$

$$\mathbf{\Gamma}_{ijkl,mnop}(t; dt) = 2^4/\{[\Delta x'_{1(i-1)} + \Delta x'_{1(i)}][\Delta x'_{2(j-1)} + \Delta x'_{2(j)}]$$

$$\cdot [\Delta x'_{3(k-1)} + \Delta x'_{3(k)}][\Delta x'_{4(l-1)} + \Delta x'_{4(l)}]\} \int_{x'_{1(i)} - [\Delta x'_{1(i-1)}/2]}^{x'_{1(i)} + [\Delta x'_{1(i)}/2]} dx'_1$$

$$\cdot \int_{x'_{2(j)} - [\Delta x'_{2(j-1)}/2]}^{x'_{2(j)} + [\Delta x'_{2(j)}/2]} dx'_2 \int_{x'_{3(k)} - [\Delta x'_{3(k-1)}/2]}^{x'_{3(k)} + [\Delta x'_{3(k)}/2]} dx'_3 \int_{x'_{4(l)} - [\Delta x'_{4(l-1)}/2]}^{x'_{4(l)} + [\Delta x'_{4(l)}/2]} dx'_4$$

$$\cdot \int_{x_{1(m)} - [\Delta x_{1(m-1)}/2]}^{x_{1(m)} + [\Delta x_{1(m)}/2]} dx_1 \int_{x_{2(n)} - [\Delta x_{2(n-1)}/2]}^{x_{2(n)} + [\Delta x_{2(n)}/2]} dx_2 \int_{x_{3(o)} - [\Delta x_{3(o-1)}/2]}^{x_{3(o)} + [\Delta x_{3(o)}/2]} dx_3$$

$$\cdot \int_{x_{4(p)} - [\Delta x_{4(p-1)}/2]}^{x_{4(p)} + [\Delta x_{4(p)}/2]} dx_4 G(\mathbf{X}', \mathbf{X}, t; dt) \tag{18}$$

where the subscripts *ijkl* and *mnop* = signature of each element in the discretized probability domain at the poststate and prestate, respectively. Eq. (18) indicates that the transition tensor is an explicit time function that needs to be updated continuously with time.

Each element of PDF at the prestate propagates through the transition tensor, and the PDF at the poststate is represented by the accumulation of all contributions from the prestate, i.e.

$$P_{ijkl}(t + dt) = \sum_{m=1}^{N_d} \sum_{n=1}^{N_d} \sum_{o=1}^{N_f} \sum_{p=1}^{N_f} \mathbf{\Gamma}_{ijkl,mnop}(t; dt) P_{mnop}(t) \tag{19}$$

Recall that there exists a reduction of velocity magnitude if PDF crosses the boundary of zero displacement ($x_1 = 0$) between the positive and negative displacement subdomains. This local velocity reduction is implemented numerically by shifting the locations of the trajectories in the probability domain. The zero crossing for a trajectory that has potential of crossing the boundary can be determined via the technique described by Yim and Lin (1991). After impact, the location of the trajectory is shifted by $(1 - e)x_2$ along x_2 axis. The angular displacement and velocity corresponding to the shifted location are then used as the initial conditions for the trajectory for the next propagation. The desired PDF is obtained by iterating (19).

Mean First-Passage Time

System performance can be evaluated by its reliability, which measures the probability of system response contained within the desired (safe) domain for a given period of time. In this case it is equal to the survival probability given by Soong and Grigoriu (1992)

$$P_s(t) = P\{T_D > t\} \tag{20}$$

where T_D = a random variable denoting the time of first-domain–outcrossing system response exceeding a given duration t. The system performance can alternatively be represented by probabilistic properties (e.g., moments) of T_D, the first-passage time, giving the time to the first exit of response out of a desired (safe) domain. Moments of any order of the first-passage time can be directly calculated as

$$E\{T_D^k\} = k \int_0^\infty t^{k-1} P_s(t)\, dt \tag{21}$$

provided that

$$\lim_{t \to \infty} \tau^k P_s(t) = 0 \tag{22}$$

The mean (first-order moment, $k = 1$) of the first-passage time, i.e., the averaged time of response escaping out of the desired domain, is used to demonstrate the system performance in this study. The survival probability P_s in (20) and (21) is obtained by numerically solving the FPE using the path-integral solution with given initial conditions and the following boundary conditions:

$$P(x_1, x_2, t) = 0 \tag{23}$$

for $x_1 > +x_{1s}$, $x_2 > 0$; $x_1 \leq -x_{1s}$, $x_2 > 0$; $x_1 \geq +x_{1s}$, $x_2 < 0$; and $x_1 < -x_{1s}$, $x_2 < 0$. Variables $\pm x_{1s}$ define the upper/lower bounds of the safe (bounded) domain for the rocking response. The bounds are closely related to the pseudo-separatrix, which is a function of damping mechanism and excitation details (Jordan and Smith 1987). For simplicity of calculation and consistency with time-domain simulations and histogram computations in Lin and Yim (1996), x_{1s} is chosen to be $\pi/2$, i.e., the rigid object is in a horizontal (overturned) position, and the resulting estimate can provide an upper bound for the mean of the first-passage time.

With the availability of survival probability (or reliability) P_s, the duration of rocking response to stochastic excitation remaining within safe domain can be estimated and demonstrated. With P_s and $E\{T_D\}$ as performance indices, sensitiv-

ity of the system response behaviors to excitation randomness parameter γ, slenderness ratio r, velocity restitution coefficient e, uncertainties in initial conditions, as well as the effects of (non)stationarity of stochastic excitation can be conducted and demonstrated in later sections.

NUMERICAL SIMULATION

Sample paths of the rocking response in a stochastic state can be obtained by directly integrating the stochastic differential equations [(5), (8), and (9)] using a fourth-order Runge-Kutta integration algorithm.

The numerical representation of the narrow-band noise selected in this study is based on Shinozuka's approach (Shinozuka 1971). The frequency range is equally divided into small segments and the corresponding strips are formed in the spectrum. The area of each strip denotes the input energy, which is equivalent to a sinusoidal excitation with a random phase shift and a random frequency with mean located at the center of the frequency segment. The total energy due to a narrow-band excitation imposed on the rocking system is equivalent to the sum of all the sinusoidal excitations. The number of sinusoidal functions is chosen 100 in this study to ensure sufficiently accurate description.

PROBABILISTIC BEHAVIORS OF ROCKING RESPONSE

The PDFs obtained by solving the FPE using the path-integral solution can provide the global information about the response behaviors. They are used in this section to examine the influence of the presence of random noise and the sensitivities of the rocking motions to various system and excitation parameters.

Finite-Amplitude and Overturning Responses

The external random noise plays a role in bridging all coexisting attracting domains. The corresponding PDFs portray these attractors on a Poincaré map and indicate their relative strengths. Fig. 1 shows the evolution of the PDFs in the first few cycles of the excitation period. The PDF is concentrated in the safe region for the first two cycles [Figs. 1(a) and (b)], and then spreads widely over the phase space after two and a half cycles [Fig. 1(c)]. As observed in Lin and Yim (1996), this behavior indicates that the domains of attractions of all coexisting attractors are bridged by the external noise. Spreading of the PDF implies that the overturning regime (diverging to $\pm\pi/2$ displacements) is a much stronger attractor compared to the other coexisting attracting domains of bounded responses (including periodic and chaotic). Thus, all the response trajectories will eventually converge to the overturning regime due to the presence of stochastic excitation.

Response Sensitivity to System Parameter Variations

The weak stability of the chaotic rocking response has been qualitatively demonstrated by the evolution of the PDF shown in the previous section. Alternatively, the stability of the stochastic rocking response can be quantitatively elucidated by its mean first-passage time, which estimates the averaged escape time of stochastic rocking responses out of the bounded domain. With this quantity as an indicator of response stability, sensitivity studies on excitation randomness parameter γ, slenderness ratio $r(H/B)$, velocity restitution coefficient e, as well as the uncertainty in the initial conditions are conducted in the following sections. Results from the following sections provide an analytical interpretation of the response stability from a reliability perspective. They also serve to qualitatively calibrate experimental and numerical simulation results obtained by previous researchers (Aslam et al. 1980; Yim et al. 1980).

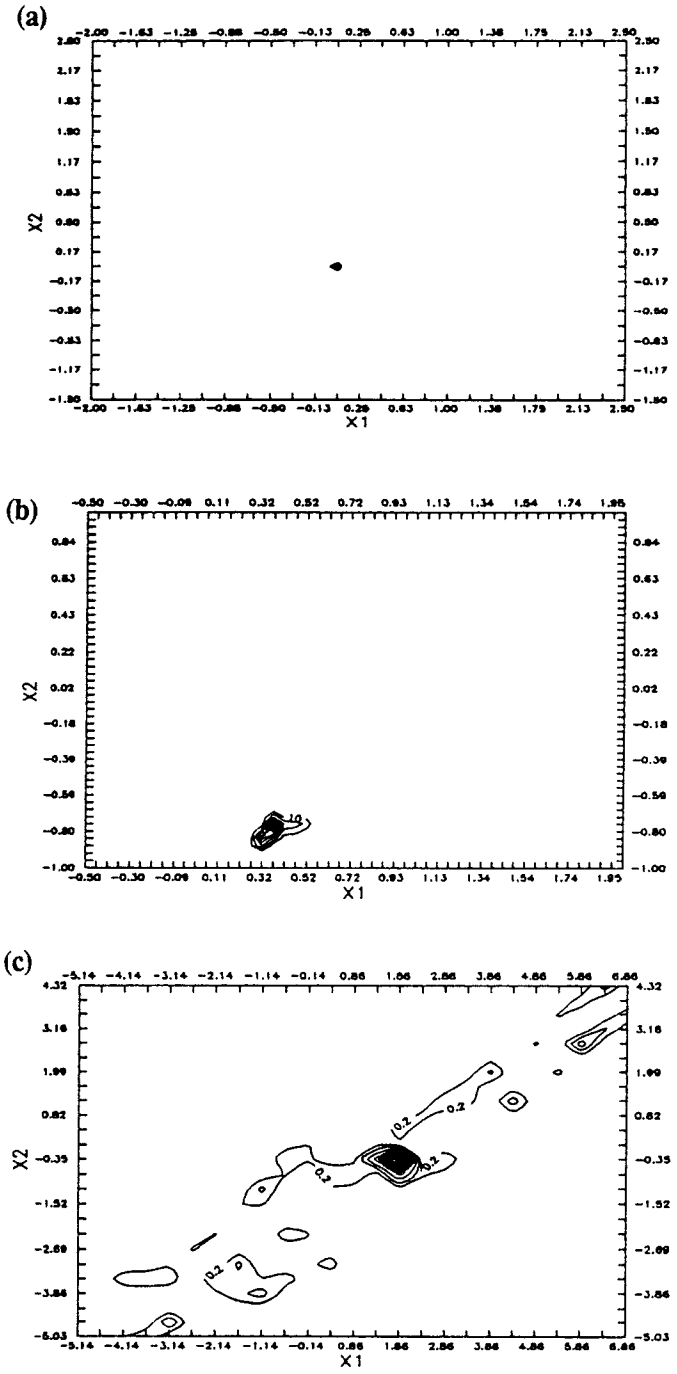

FIG. 1. Evolution of PDF: (a) Initial Probability Concentrated at (0.0, 0.0); (b) Probability Density at First Cycle of Forcing Period; (c) Probability Density after 2.5 Cycles of Forcing Period (Overturning Occurs) [(a, ω, r, e, α, γ, ϕ) = (14.7, 2.7, 10, 0.5, 1.0, 0.95, 0.0)]

Excitation Randomness Parameter γ

Sensitivity of the rocking response to the degree of randomness in excitation can be examined by varying the randomness parameter γ in the range of [0 1] (from purely random to purely deterministic). The total energy, due to combined deterministic and stochastic components, injected into the system remains constant and is equal to the level that could cause chaotic response in the deterministic setting. In this manner, close relationships between chaotic and overturning responses can be demonstrated. The system performance is evaluated and

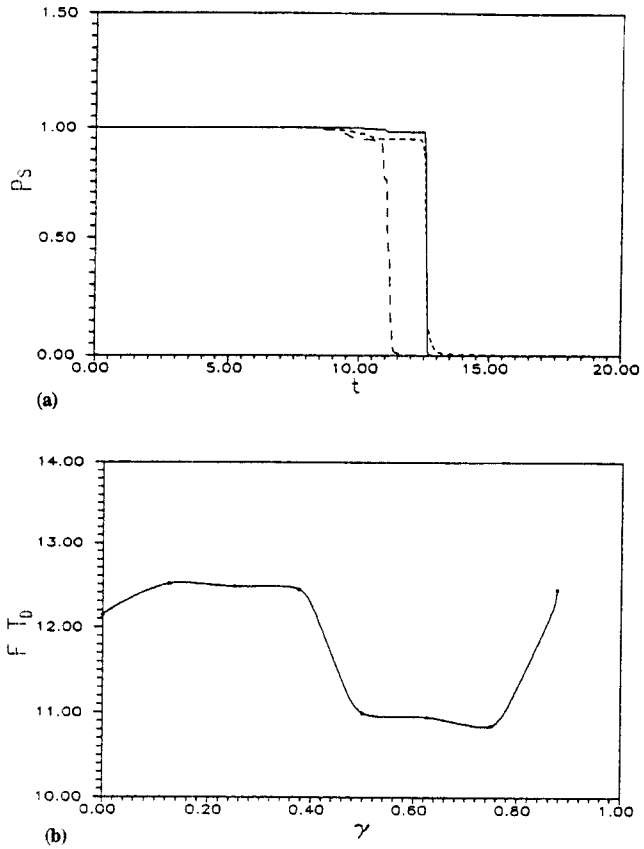

FIG. 2. Sensitivity of Rocking Response to Various Degree of Stochasticity of Excitation: (a) Survival Probability versus Time (Solid, Short-Dashed, and Long-Dashed Lines for Cases with γ = 0.125, 0.375, and 0.75, Respectively); (b) Mean First-Passage Time versus Excitation Parameter γ [(a, ω, r, e, α, ϕ) = (14.7, 2.7, 10, 0.5, 1.0, 0.0)]

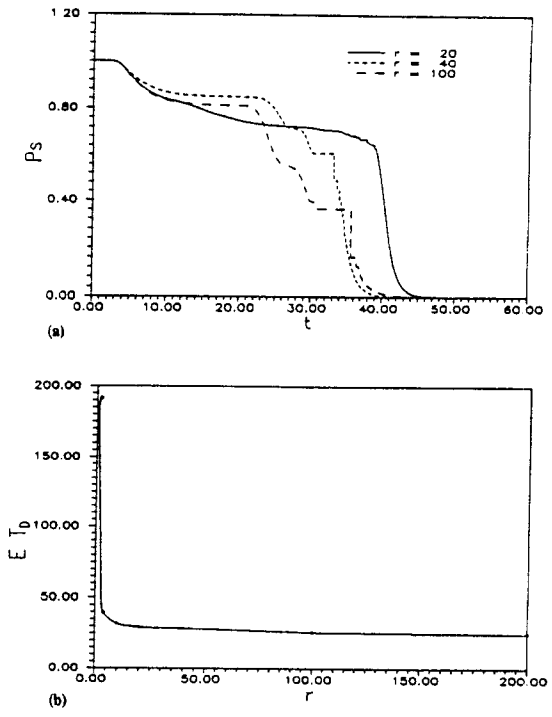

FIG. 3. Sensitivity of Rocking Response to Various Slenderness Ratios (H/B): (a) Survival Probability versus Time; (b) Mean First-Passage Time versus R [(a/θ_{cr}, ω, e, R, γ, ϕ) = (147, 2.7, 0.5, 290, 0.0, 0.0)]

illustrated by the corresponding survival probability (or reliability) and mean first-passage time.

Fig. 2(a) shows the survival probabilities as a function of time for rocking response with various degrees of stochasticity in the excitation (γ = 0.125, 0.375, and 0.75). It indicates that the stability of the response decreases when parameter γ increases. This is caused by the fact that, with the same energy level, the response trajectories in the safe domain can be easily driven toward the safe/overturning boundary by a large-amplitude periodic component in the excitation, thus overturning may follow.

A more detailed sensitivity study of response to randomness parameter is presented in Fig. 2(b), which shows the mean first-passage time as a function of randomness parameter γ. In the range of between 0 and 0.4, Fig. 2(b) shows that mean first-passage time is relatively constant as γ increases. However, there is a drop at about 0.45 as γ increases, which may indicate that when the periodic excitation amplitude reaches such a level (γ = 0.45), it promptly drives the response out of the safe domain. The mean first-passage time again state at a relatively constant level between γ = 0.5 to 0.76. An increase is also observed for γ above 0.8. This is likely caused by the phenomenon called "noise-induced chaos." In this region, the stable and unstable manifolds intersect and the domain of bounded response is expanded 1.55 times of the static critical angle [see Lin and Yim (1996)]. Moreover, because of such an expansion of safe domain, the duration of response trajectories staying the expanded domain increases, so does the mean first-passage time. This increasing trend will continue as randomness parameter γ approaches 1.0. At this limit, the rocking response falls into a stable deterministic chaotic attractor, and the corresponding mean first-passage time becomes infinite.

Slenderness Ratio r

The geometry as well as physical dimension of the rigid block for a given base width are characterized by the slenderness ratio r and radius of gyration R. It has been observed that for a given geometric portion, larger blocks are more stable than smaller ones (Aslam et al. 1980; Yim et al. 1980). In this section, rocking responses of various geometric portions (varying slenderness ratio with base width fixed) to combined deterministic and stochastic excitations (γ = 0.5, total input energy normalized with respect to the critical angle) are examined.

Fig. 3(a) shows the reliability of rocking responses with slenderness ratios r = 20, 40, and 100, respectively. It is observed that even though the mass and dimension of the rigid block increase with increasing slenderness ratio r, the corresponding response reliability decreases. A more detailed examination of the response sensitivity to slenderness ratio is demonstrated in Fig. 3(b). Dots in Fig. 3(b) are actual numerical results (varying r from 2 to 200) and the solid line is the corresponding polynomial interpolation to illustrate a trend. A drastic drop for r within the range of 2–4 and almost flat for r larger than 10 are observed. This indicates that, in the study of response reliability, slenderness (piecewise linear) assumption is adequate when r is larger than 10. It is also demonstrated that the mean first passage time of rocking response subjected to combined deterministic and stochastic excitations decreases with increasing mass and dimension of the object (width fixed), which is in line with experimental results observed by Aslam et al. (1980).

Velocity Restitution Coefficient e

The energy dissipation mechanism of the rocking system is governed by impact at zero angular displacement, which is characterized by the velocity restitution coefficient e. Chaotic response has only been observed with high energy dissipation

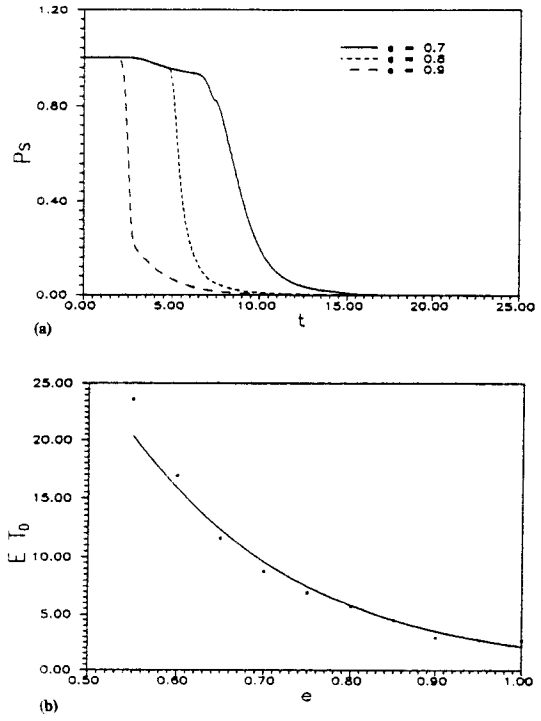

FIG. 4. Sensitivity of Rocking Response to Variations of Velocity Restitution Coefficient *e*: (a) Survival Probability versus Time; (b) Mean First-Passage Time versus *E* [(*a*, ω, *r*, α, γ, φ) = (14.7, 2.7, 10, 1.0, 0.0, 0.0)]

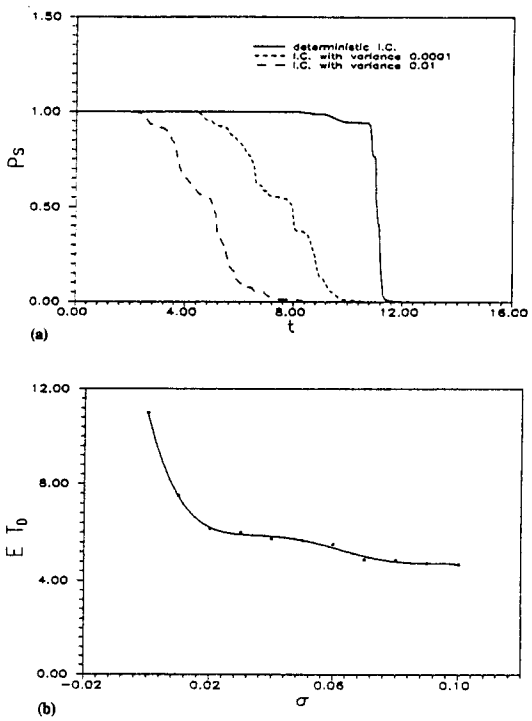

FIG. 5. Sensitivity of Rocking Response to Various Random Initial Conditions: (a) Survival Probability versus Time; (b) Mean First-Passage Time versus Standard Deviation of Initial Uncertainty [(*a*, ω, *r*, *e*, α, γ, φ) = (14.7, 2.7, 10, 0.5, 1.0, 0.5, 0.0)]

(*e* = 0.5) (Hogan 1989; Yim and Lin 1992). Such energy dissipation is probably higher than those identified in practice. Such a high velocity reduction does provide strong enough nonlinearity (together with large periodic excitation) for chaotic response. On the other hand, as indicated among the existing literature, the restitution coefficient is within the range around 0.925 (Aslam et al. 1980). Nevertheless, in this study, a wide range of *e* is studied, i.e., from 0.5 to 1.0, to examine its effects on the rocking response subjected to purely stochastic excitation (γ = 0.0).

Fig. 4(a) shows the associated reliability of rocking responses subjected to stochastic excitation with various velocity restitution coefficients (*e* = 0.5, 0.75, and 0.95). It is obvious that response reliability decreases with increasing *e*. Sensitivity of rocking responses to various degrees of damping dissipation is demonstrated in Fig. 4(b) by plotting the mean first-passage time as a function of restitution coefficient *e* from 0.5 to 1.0. As anticipated, numerical results show that the survival time decreases with increasing value of *e*.

Initial Conditions

So far all the rocking responses examined are with the quiescent initial conditions. Exactness of such initial conditions cannot be realized in practice. Imperfections in prescribing initial position can be approximated by random state variables (i.e., x_{1o} and x_{2o}). A Gaussian distribution is assumed here to describe the initial randomness. Sensitivity to such disturbance is examined by varying the variance of initial distribution, for fixed slenderness ratio (*r* = 10) and degree of stochasticity of excitation (γ = 0.5).

Fig. 5(a) shows examples of survival probabilities with various randomness in the initial conditions. It shows that stability of rocking response decreases with increasing initial uncertainties. A more detailed study of the sensitivity of the response to variations in initial conditions is carried out through averaged survival time [Fig. 5(b)] over the range of $[0.0\ 0.1^2]$. A significant drop in the mean first-passage time is observed when the variance increases from 0 to 0.02^2. The effects of initial randomness on response stability in the range of $[0.02^2\ 0.10^2]$ are observed to be much less significant.

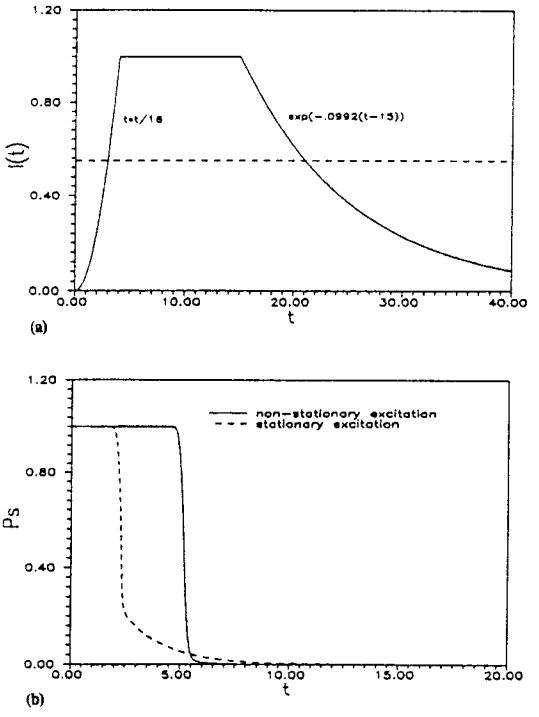

FIG. 6. Rocking Responses to Stationary and Nonstationary Excitations, Respectively: (a) Intensity-Time Functions (Solid Line for Time Varying and Dashed Line for Equivalent Time Invariant); (b) Corresponding Survival Probabilities versus Time [(*a*, ω, *r*, *e*, α, γ, φ) = (4.7, 2.7, 10, 0.925, 1.0, 0.0, 0.0)]

Response Sensitivity to (Non)Stationarity of Stochastic Excitation

So far, the stochastic excitation exerted on the rocking object has been assumed stationary. The influence of nonstation-

arity of the stochastic excitation on the rocking response can also be examined by a systematic analysis procedure demonstrated in this section. Among natural hazards, earthquakes are one of the most prominent nonstationary loading on structures that is of great interest to civil engineers. Thus, earthquake-type excitations are employed here to demonstrate the applicability of the analysis procedure to identify the influence of nonstationarity on rocking response behaviors.

Fig. 6(a) shows a typical intensity-time function characterizing acceleration of ground motion during earthquakes (Yim et al. 1980). The solid line represents the ground acceleration intensity, which increases quadratically for the first 4 s, reaches a steady state for 11 s, and finally dies out exponentially. An equivalent stationary excitation over 40 s ground motion is shown by the dashed flat line. The intensity of the equivalent stationary excitation is obtained by averaging the total area under the intensity-time function over a 40 s duration. Corresponding mean first-passage times of rocking responses subjected to nonstationary excitation and to equivalent stationary excitation are shown in Fig. 6(b). It is observed that nonstationarity of the stochastic excitation has significant influence on the response stability. Compared to the response to nonstationary excitation with the same total input energy, rocking responses are less stable under equivalent stationary excitation, thus stationary results are generally (except in the tail) more conservative.

CONCLUDING REMARKS

The rocking behaviors of rigid objects have been examined to gain a better understanding of the sensitivity and stability of the response behavior. Rocking responses of fully nonlinear rocking systems subjected to combined deterministic and stochastic excitations of arbitrary relative intensity ratios have been demonstrated from a probabilistic perspective. Based on the observed semianalytical solutions of the FPE and numerical simulation results, the following concluding remarks are offered:

1. The Fokker-Planck equation and its semianalytical solver (path-integral solution) can provide a probabilistic description of the rocking response behaviors to combined deterministic and stochastic excitations. Impact-induced energy loss is numerically implemented by incorporating a reduction in the rotational velocity when response trajectories cross zero angular displacement.
2. The resulting probability density functions provide global information about the response behaviors and the relative strengths of various attractors. The fast-spreading probability density function to overturning ($\pm\pi/2$ angular displacements) being observed indicates that overturning response is the attractor with greatest relative stability compared to the other bounded (periodic and chaotic) responses. Thus, the long-term rocking response behavior is inherently unstable when stochastic excitation is present.
3. Domains of attraction of all coexisting responses are bridged by the presence of stochastic excitations. Among coexisting response attractors, the overturning attractor is of the greatest strength. Hence, as observed in Lin and Yim (1996), semianalytical results obtained in this study demonstrate that a rocking object will overturn eventually with stochastic excitation present. Thus, it may be difficult to identify the existence of transient chaotic rocking response in a stochastic state by examining time histories alone.
4. Rocking system performance in terms of reliability have been examined and demonstrated by the mean first-passage time, which provides a quantitative representation of the response stability. For a given rocking system, a more stable response is indicated by a larger value of mean first-passage time. This systematic analysis procedure can also be applied to rocking responses subjected to nonstationary excitation.
5. Sensitivity studies of the response to relative randomness parameter γ, system slenderness ratio r, velocity restitution coefficient e, as well as uncertainties in initial conditions have been conducted using the mean first-passage time as a performance index. It is observed that the reliability of rocking response decreases with increasing randomness, however, when γ approaches unity (near chaotic domain), because of expansion of the safe region, the reliability increase rapidly. It is also observed that the reliability of rocking response decreases with increasing slenderness ratio r even with the associated increases in mass and physical dimension of the block. The system behavior becomes less reliable with the increase of restitution coefficient e or uncertainties in initial conditions.
6. The effects of nonstationarity is shown to be significant. Compared to the response of nonstationary excitation with the same total input energy, rocking responses are less stable under equivalent stationary excitation.

ACKNOWLEDGMENT

The writers gratefully acknowledge the financial support from the United States Office of Naval Research (grant No. N00014-92-J-1221).

APPENDIX I. REFERENCES

Aslam, M., Godden, W. G., and Scalise, D. T. (1980). "Earthquake rocking response of rigid bodies." *J. Struct. Engrg. Div.*, ASCE, 106(2), 377–392.

Dimentberg, M. F., Lin, Y. K., and Zhang, R. (1993). "Toppling of computer-type equipment under base excitation." *J. Engrg. Mech. Div.*, ASCE, 119(1), 145–160.

Hogan, S. J. (1989). "On the dynamics of rigid-block motion under harmonic forcing." *Proc., Royal Soc. London A*, London, England, 425, 441–476.

Iyengar, R. N., and Manohar, C. S. (1991). "Rocking response of rectangular rigid blocks under random noise base excitations." *Int. J. Nonlinear Mech.*, 26, 885–892.

Jordan, D. W., and Smith, P. (1987). *Nonlinear ordinary differential equations*. Oxford University Press, Oxford, England.

Koh, A. S. (1986). "Rocking of rigid blocks on randomly shaking foundations." *Nuclear Engrg. and Des.*, 97, 269–276.

Lin, H., and Yim, S. C. S. (1996). "Nonlinear rocking motions. I: chaos under noisy periodic excitations." *J. Engrg. Mech.*, ASCE, 122(8), 719–727.

Risken, H. (1984). *The Fokker-Planck equation: methods of solution and applications*. Springer-Verlag, Berlin, Germany.

Shinozuka, M. (1971). "Simulation of multivariate and multidimensional random processes." *J. Acoustical Soc. of Am.*, 49, 357–367.

Soong, T. T., and Grigoriu, M. (1992). *Random vibration of mechanical and structural systems*. Prentice-Hall, Englewood Cliffs, N.J.

Spanos, P. D., and Koh, A. S. (1986). "Analysis of block random rocking." *Soil Dyn. and Earthquake Engrg.*, 5, 178–183.

Stratonovich, R. L. (1967). *Topics in the theory of random noise I*. Gordon and Breach, New York, N.Y.

Wehner, M. F., and Wolfer, W. G. (1983). "Numerical evaluation of path-integral solutions to Fokker-Planck equations." *Physical Rev. A*, 27, 2663–2670.

Wissel, C. (1979). "Manifolds of equivalent path integral solutions of the Fokker-Planck equation." *Zeitschrift für Physiks B*, Germany, 35, 185–191.

Yim, S. C. S., Chopra, A. K., and Penzien, J. (1980). "Rocking response of rigid blocks to earthquakes." *Earthquake Engrg. and Struct. Dyn.*, 8, 565–587.

Yim, S. C. S., and Lin, H. (1991). "Chaotic behavior and stability of free-standing offshore equipment." *Oc. Engrg.*, 18, 225–250.

Yim, S. C. S., and Lin, H. (1992). "Probabilistic analysis of a chaotic dynamical system." *Applied chaos*, J. H. Kim and J. Stringer, eds., John Wiley & Sons, New York, N.Y., 219–241.

APPENDIX II. NOTATION

The following symbols are used in this paper:

a = periodic excitation amplitude (lb-in.);
B = object width (in.);
e = velocity restitution coefficient;
f = filtered white noise;
G = short-time probability density function;
H = object height (in.);
I_0 = mass moment of inertia (lb-in.-sec^2);
$I(t)$ = intensity-time function;
M = object mass (slug);
$P(\mathbf{X}, t)$ = probability density function;
$P_s(t)$ = survival probability or reliability;
R = radius of rotation;
r = slenderness ratio;
t = time (s);
T_D = first-passage time (s);
$\mathbf{X}$ = state vector;
β = linear filter bandwidth parameter;
$\mathbf{\Gamma}$ = short-time transition tensor;
γ = excitation parameter;
θ = angular displacement (rad);
θ_{cr} = critical (static overturning) angle (rad);
κ = noise intensity;
ξ = ideal white noise;
ϕ = phase shift of periodic excitation;
Ω_o = linear filter natural frequency (rad/s); and
ω = periodic excitation frequency (rad/s).